Single-pulse writing of a concave microlens array

Xiao-Wen Cao,[1] Qi-Dai Chen,[2,6] Lei Zhang,[1] Zhen-Nan Tian,[2] Qian-Kun Li,[2] Lei Wang,[2] Saulius Juodkazis,[4,5,7] and Hong-Bo Sun[2,3,8]

[1]State Key Laboratory of Integrated Optoelectronics, School of Mechanical Science and Engineering, Nanling Campus, Jilin University, Changchun 130025, China
[2]State Key Laboratory of Integrated Optoelectronics, College of Electronic Science and Engineering, Jilin University, Changchun 130012, China
[3]State Key Laboratory of Precision Measurement Technology and Instruments, Department of Precision Instrument, Tsinghua University, Haidian, Beijing 100084, China
[4]Centre for Micro-Photonics, Faculty of Science, Engineering and Technology, Swinburne University of Technology, Hawthorn, VIC 3122, Australia
[5]Melbourne Centre for Nanofabrication, ANFF, 151 Wellington Road, Clayton VIC 3168, Australia
[6]e-mail: chenqd@jlu.edu.cn
[7]e-mail: sjuodkazis@swin.edu.au
[8]e-mail: hbsun@tsinghua.edu.cn

This work developed a method of femtosecond laser (fs-laser) parallel processing assisted by wet etching to fabricate 3D micro-optical components. A 2D fs-laser spot array with designed spatial distribution was generated by a spatial light modulator. A single-pulse exposure of the entire array was used for parallel processing. By subsequent wet etching, a close-packed hexagonal arrangement, 3D concave microlens array on a curved surface with a radius of approximately 120 µm was fabricated, each unit lens of which has designable spatial distribution. Characterization of imaging was carried out by a microscope and showed a unique imaging property in multi-planes. This method provides a parallel and efficient technique to fabricate 3D micro-optical devices for applications in optofluidics, optical communication, and integrated optics. © 2018 Optical Society of America

Microlens arrays (MLAs) have been proven to be important and irreplaceable optical devices due to their capability of integration, small volume, low cost, and distinctive optical performance in expanding the number of applications in microfabrication [1,2], 3D displays [3], beam shaping [4,5], and integrated optofluidic microchips [6]. Various methods have been proposed for fabrication of MLAs, such as laser direct writing (LDW) [7,8], thermal photoresist reflow [9], droplet inkjet [10], grayscale lithography [11], and multi-beam interference [12]. However, these methods are suitable only for soft materials, which limits the usage of MLAs in extreme environments. To overcome this deficiency, a maskless method by femtosecond (fs-)laser assisted local wet etching was proposed and

used for fabrication of micro-optics devices on silica glasses [13]. The size and arrangement of the MLAs can be easily adjusted by etching time and control of laser exposure conditions as revealed by exploration of parameter space of this method [14–16]. The MLA could be fabricated on both plane [13,15,16] and curved surfaces [14,17]. However, most of the methods were carried out with dot-by-dot, which limited the processing flexibility and efficiency.

Herein, a method of fs-laser parallel processing assisted by etching to fabricate a 3D concave microlens array (CMLA) on silica was proposed, combining fs-laser pulse parallel irradiation and wet etching. The productivity could be improved obviously with parallel processing [18]. The laser beam is divided into the required pattern of beamlets with a spatial light modulator (SLM) [19], which modulates beams amplitude and phase [20,21]. With SLM, a beam irradiation was split into multi-spots with controlled position and energy, which were adjustable individually. A designed dot array was obtained by ablation with the split fs-laser pulse [22,23]. After being etched, the exposed/ablated dot array was evolving into a micro-concave lens pattern, in which each unit lens size was controlled by the corresponding exposure dose controlled individually. Thus, a complex micro-concave lens array, including 3D arrangement, could be obtained through one-pulse-shot irradiation and subsequent wet etching. This method provides a parallel and efficient technique to fabricate complex 3D close-packed compound micro-optical arrays for demanding imaging applications.

In our experiments, a holographic fs-laser processing system, schematically shown in Fig. 1(a), was used. Laser pulses from a fs-laser amplifier (Pharos PH1-SP-1mJ, Light Conversion Ltd.) with center wavelength of 1028 nm, pulse duration of 190 fs, repetition rate of 200 kHz, and maximum pulse energy of 1 mJ were frequency doubled by a nonlinear-optical beta-barium borate (BBO) crystal to obtain 514 nm wavelength and to eliminate a long ns-pulse pedestal. Then, the diameter of the laser beam was expanded three times through a telescope using focal

lengths of −50 mm and 150 mm lenses. The expanded beam irradiated on a reflection and phase-only liquid crystal-on-silicon spatial light modulator (LCOS-SLM, LETO, HOLOEYE Photonics AG) for phase modulation. It provides 256 (8-bit) phase levels and full high definition (FHD) over 1920 × 1080 pixels area. The pixel pitch was 6.4 μm with interpixel gap of 0.2 μm, so it can provide a high fill factor of 93% and a high light efficiency. The maximum available power density up to ~2 W/cm² can be accommodated. The transformed multi-beamlets pattern after SLM was transferred to the entrance of a plan objective with numerical aperture (NA) of 0.7 by a 4-f optical system, which was composed of two plano-convex lenses with focal lengths of 400 mm and 300 mm. Finally, the pattern of multiple beams was focused on the surface of the sample, resulting in multiple focal spot irradiation. Each spot's energy was controlled by SLM defining a circle size, as shown in Fig. 1(b). The sample was fixed on a motorized linear *x-y* stage powered by a step motor with resolution of 100 nm and maximum stroke of 20 mm. Focusing was controlled with a piezo *z* stage with resolution of 1 nm and maximum stroke of 100 μm. The computer generated hologram [(CGH) with resolution of 1024 × 1024, shown in Fig. 1(c)] was generated using the optimal rotation angle (ORA) method [24]. Usually, the 0th-order light always exists because the modulation efficiency of the SLM is not 100%, and its intensity can be large enough to ablate the sample [25] even when ablation threshold is high [26]. The 0th-order light can be isolated in *z* direction [27] or *x-y* plane [28] to remove its unwanted influence. As shown in Figs. 1(c)–1(e), we applied a spherical phase factor that allowed to separate (10 μm) the multiple focal spots from the 0th-order light in *z* direction. When these beamlets were focused on the surface of the sample, the 0th-order light was focused far from the surface, and unwanted ablation was avoided. Finally, the sample was etched in 20% vol. aqueous hydrogen fluoride (HF) solution at room temperature of 25°C. The micro-concave lens array was obtained after time-controlled etching. A laser confocal microscope (LSCM, LEXT OLS4100, Olympus) was used to measure the lens's size, including width, depth, and the curvature radius.
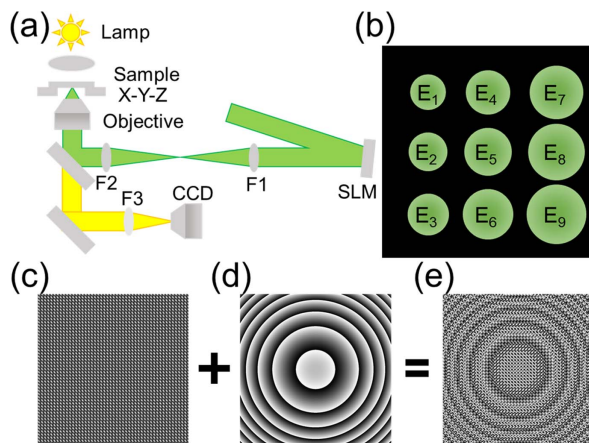

Fig. 1. (a) Schematic of holographic femtosecond laser processing system with SLM. (b) Sketch of nine focal spots with different pulse energies. (c) Computer-generated hologram (CGH) generated by ORA method using pattern shown in (b). (d) Spherical phase factor for defocusing of 0th order beam. (e) Multi-unit CGH made by combination of (c) and (d).
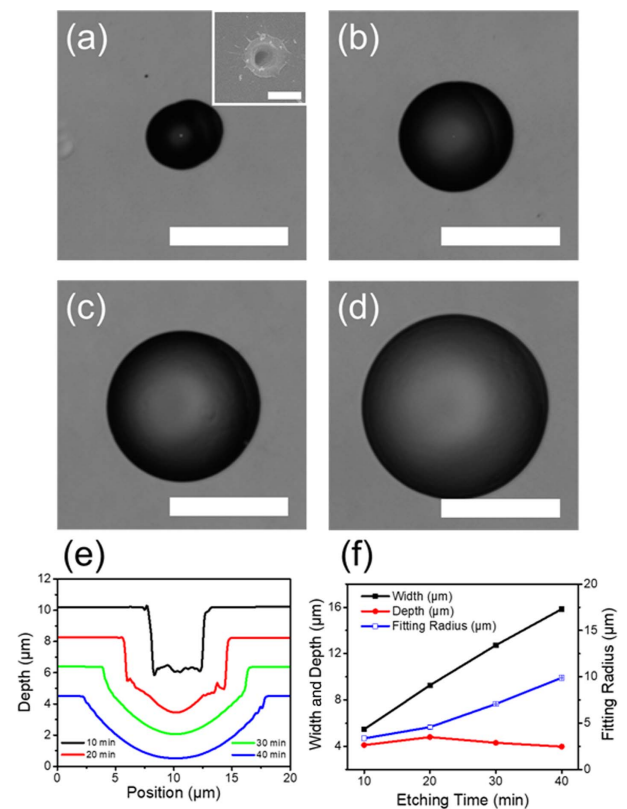

Fig. 2. Formation process of a micro-concave lens. The SEM image of a seed ablation dent induced by a single fs-laser pulse with pulse energy of 135 nJ [inset of (a)]. (a)–(d) Top view of the structure after being etched for 10, 20, 30, and 40 min, respectively. (e) Shapes of the depth cross section correspond to (a)–(d). (f) Width, depth, and curvature radius of the structure vary with etching time. Scale bar: 10 μm (a)–(d), 1 μm [inset of (a)].

The process of fabrication of a micro-concave lens on silica flat surface was investigated first. A single fs-laser pulse with energy of 135 nJ (with peak irradiance 1.13×10^{14} W/cm² [29]) was focused on the silica surface, inducing an ablation pit acting as a seed dent for etching, as shown in the inset of Fig. 2(a). The seed dent was a sub-micrometer-sized ablation crater. Melted silica was thermally quenched around the ablation crater [30,31]. The modification was well defined and localized without damage of surroundings, as revealed by SEM. Interestingly, the etch rate of those surrounding regions was faster than that of unmodified areas when immersed in the HF solution. The mechanism was discussed in detail by Marcinkevicius's work [32]. The top view of the structure after etching for 10, 20, 30, and 40 min is shown in Figs. 2(a)–2(d). After a short etching time of 10 min, the modified region was etched first, and the outline was elliptic [Fig. 2(c)], because the focal spot was not a perfect circle. Meanwhile, the cross section showing the depth of the etched pit was rectangular [Fig. 2(e)]. The diameter of the etched structure was 5.5 μm, which was approximately twice larger than the diameter of the focal spot (approximately 1.8 μm). As a result, we could conclude that the region directly modified by the laser pulse was thoroughly removed. After etching for 20 min, the bottom of the structure was evolving into a spherical shape, but the side wall was still vertical due to the isotropic nature of the etching process [33].

The outline of the depth cross section was turning into a spherical profile with etching time. The diameter of the structure was changed from 5.5 µm to 9.3 µm with etching time increased by 10 min. Therefore, we could calculate that the etching rate of fused quartz in HF solution (20%) was 190 nm/min. For longer etching times, the bottom spherical profile was expanding laterally reducing the section of the vertical side wall. After 40 min, the vertical side wall disappeared, as shown in Fig. 2(e). The structure was finally evolving into a perfect micro-concave lens, as shown in Fig. 2(d). The width and depth of the lens were 15.8 µm and 4.0 µm, respectively. Its curvature radius was 9.4 µm.

Because of the isotropic nature of the etching process, the curvature radius and the width of structure increased with etching time, while the depth remained unchanged, as shown in Fig. 2(f). Thus, the focal length of the lens can be adjusted easily through etching time, as it had a linear relationship with the radius. Furthermore, the surface of the structure became smoother with etching time. After 40 min, the roughness of the structure was less than 10 nm (measured with LSCM), as shown in Fig. 2(d).

A seed induced by the fs-laser pulse evolved into a perfect micro-concave lens after being etched for 40 min.

In the same wet etching conditions, the size of the lens could be controlled with laser pulse energy. Herein, the relationship between the size/diameter of the micro-concave lens and laser pulse energy was investigated using a novel and simple method. Utilizing the SLM and ORA methods, a beam irradiation was split into a nine-spot array with relative energy from 0.6 to 1, and the schematic is shown in Fig. 1(b). The distance between each spot was set at 20 µm, and the pulse energies of each spot were set from 84 nJ to 243 nJ. The nine spots with single pulse were irradiated on the silica surface, and then a nine-seed array was obtained at one time, as shown in Fig. 3(a). The energy distribution had the same ellipsoidal shape at the focus and affected the shape of the etched pit at the initial stage. Irradiated by larger pulse energy, the modified region was larger, as shown in Fig. 3(b). The sizes of the modified region were from 1.0 µm to 1.4 µm. Subsequently, the sample was etched in HF (20%) for 40 min and a micro-concave lens array was obtained, as shown in Fig. 3(c). Each lens had designable size. The surface qualities of all these lenses were the same and with perfectly smooth surfaces. The cross section of each lens [Fig. 3(d)] showed that each lens had an approximate spherical profile.

With the same etching time, the size of the micro-concave lens depended on the modified region's size. The width was changed from 15.0 µm to 17.5 µm, and the depth was changing from 3.0 µm to 5.0 µm. Figure 3(e) shows that both the height and width increased with pulse energy. Furthermore, the curvature radius of the micro-concave lens was measured, and the relationship between it and pulse energy was investigated. The curvature radius was independent of pulse energy. With pulse energy varying from 84 nJ to 243 nJ, the curvature radius, R, was constant at 9.5 ± 0.15 µm. The focal length of the lens can be described by the formula

$$f = -\frac{R}{n-1},\tag{1}$$

where $n = 1.46$ is the refractive index of the fused quartz, and f is the focal length. The minus sign means that the concave lens has a virtual focus. As a result, the focus length was -20.7 ± 0.3 µm, independent of pulse energy, as shown in Fig. 3(f).
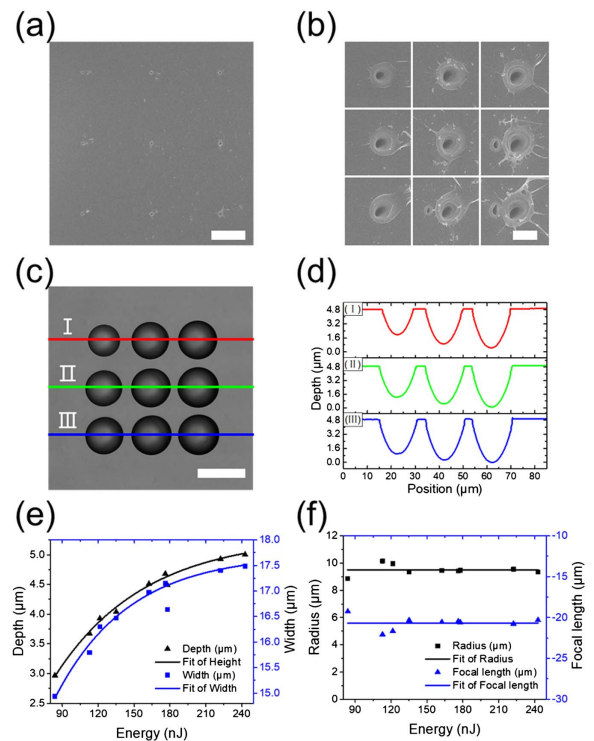

Fig. 3. (a) Nine-seed array induced by a single fs-laser pulse with relative energy from 0.6 to 1 and its zoomed-in view (b). (c) Top view of the microlens array, consisting of nine microlenses with different focal lengths. (d) Side view of each micro-concave lens. (e) Depth and width of the lens versus the pulse energy. (f) Curvature radius and the focal length versus the pulse energy.

Finally, a complex dot array with a hexagonal arrangement consisting of a pre-designed pulse energy exposure was generated, as shown in the insert of Fig. 4(a). A beam with pulse energy of 7.1 µJ was irradiated on the SLM. The energy per each spot was defined by the circle size on SLM. The relative energies were set at 1, 0.9, 0.8, and 0.7 from the center to the outside. Separation between each spot was 10 µm. As mentioned before, after being etched for 40 min, the width of the micro-concave lens was larger than 10 µm. Therefore, these lenses formed a close-packed pattern of a 3D compound lens with radius of approximately 120 µm. Figures 4(b) and 4(c) show the 3D topography and side view of the compound lens, respectively. The position shift in z direction was about 4 µm between the most off-center and the center lenses. The curvature radii of these lenses were the same. As a result, the focal spot was determined only by the z position.

The imaging performance of this array was demonstrated with a microscope, as shown in Fig. 4(d). The imaging showed a varying focusing performance via adjusting the distance between the objective and the sample, as shown in Figs. 4(e) and 4(f). The green box shows the imaging performance of the center lens and the red box for the off-center lens. While the center lens shows a clear image, the outside lenses show blurred out-of-focus images. Conversely, while the outside lenses showed clear, crisp images, the center lens was out of focus. This shows that this compound lens could get a clear image in a series of z positions. This has an application
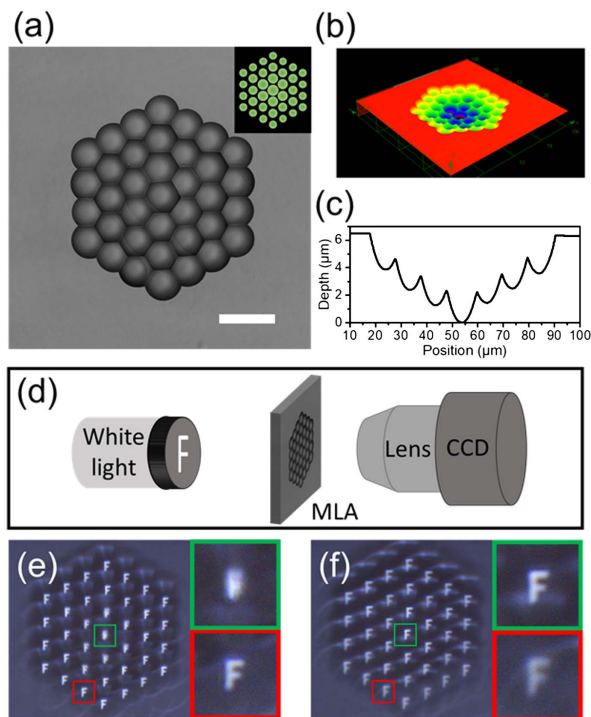
Fig. 4. (a) Top view of the close-packed compound microlens with 3D arrangement. The inset shows the corresponding light distribution. Scale bar is 20 μm. (b) and (c) were the 3D topography and side view of the micro-concave lens in (a). (d) Schematic of the imaging system for MLA. (e, f) Imaging performance of compound MLA, out-of-center (e), and center (f) show clear images, respectively.

potential in optofluidics, optical communication, integrated optics, and inspection imaging of moving objects on production lines.

In summary, we have introduced a parallel and efficient method to fabricate 3D MCLA using fs-laser parallelly induced ablation and wet etching in HF solution (20%). The micro-lens topography was varying with etching time and provides control over diameter of separate micro-lenslets. The relationship between single-lens width, depth, and curvature radius, and pulse energy was established. A complex 3D compound micro-concave lens with close-packed hexagonal arrangement on curved surface with radius of approximately 120 μm was fabricated, using a phase-only SLM to modulate the laser beam. This array had a good imaging performance in various planes, depending on the lateral location of the lenslets. Application potential spans areas of micro-optics, optical communication, and integrated optics. Above all, this method could fabricate any designed arrangement of micro-concave lens arrays, including 2D and 3D, through changing patterns defined by CGH, with single-pulse irradiation and being etched for the same time duration. This provided a parallel and efficient tool to fabricate 3D micro-optical devices, which has potential application in optofluidics, optical communication, and integrated optics.

REFERENCES

1. S. Matsuo, S. Juodkazis, and H. Misawa, Appl. Phys. A **80**, 683 (2005).
2. S. Matsuo, T. Miyamoto, T. Tomita, and S. Hashimoto, Appl. Opt. **46**, 8264 (2007).
3. P.-A. Blanche, A. Bablumian, R. Voorakaranam, C. Christenson, W. Lin, T. Gu, D. Flores, P. Wang, W.-Y. Hsieh, and M. Kathaperumal, Nature **468**, 80 (2010).
4. Y. Jin, A. Hassan, and Y. Jiang, Opt. Express **24**, 24846 (2016).
5. Z. Deng, Q. Yang, F. Chen, X. Meng, H. Bian, J. Yong, C. Shan, and X. Hou, Opt. Lett. **40**, 1928 (2015).
6. D. Wu, J. Xu, L.-G. Niu, S.-Z. Wu, K. Midorikawa, and K. Sugioka, Light Sci. Appl. **4**, e228 (2015).
7. Z.-N. Tian, W.-G. Yao, J.-J. Xu, Y.-H. Yu, Q.-D. Chen, and H.-B. Sun, Opt. Lett. **40**, 4222 (2015).
8. D. Wu, S.-Z. Wu, L.-G. Niu, Q.-D. Chen, R. Wang, J.-F. Song, H.-H. Fang, and H.-B. Sun, Appl. Phys. Lett. **97**, 031109 (2010).
9. X. Li, Y. Ding, J. Shao, H. Liu, and H. Tian, Opt. Lett. **36**, 4083 (2011).
10. S. Nagelberg, L. D. Zarzar, N. Nicolas, K. Subramanian, J. A. Kalow, V. Sresht, D. Blankschtein, G. Barbastathis, M. Kreysing, and T. M. Swager, Nat. Commun. **8**, 14673 (2017).
11. J.-J. Yang, Y.-S. Liao, and C.-F. Chen, Opt. Commun. **270**, 433 (2007).
12. S. Behera and J. Joseph, Opt. Lett. **41**, 3579 (2016).
13. F. Chen, H. Liu, Q. Yang, X. Wang, C. Hou, H. Bian, W. Liang, J. Si, and X. Hou, Opt. Express **18**, 20334 (2010).
14. G. Du, Q. Yang, F. Chen, H. Liu, Z. Deng, H. Bian, S. He, J. Si, X. Meng, and X. Hou, Opt. Lett. **37**, 4404 (2012).
15. X. Meng, F. Chen, Q. Yang, H. Bian, H. Liu, P. Qu, Y. Hu, J. Si, and X. Hou, IEEE Photon. Technol. Lett. **25**, 1336 (2013).
16. S. Tong, H. Bian, Q. Yang, F. Chen, Z. Deng, J. Si, and X. Hou, Opt. Express **22**, 29283 (2014).
17. H. Bian, Y. Wei, Q. Yang, F. Chen, F. Zhang, G. Du, J. Yong, and X. Hou, Appl. Phys. Lett. **109**, 221109 (2016).
18. L. Wang, Q.-D. Chen, X.-W. Cao, R. Buividas, X. Wang, S. Juodkazis, and H.-B. Sun, Light Sci. Appl. **6**, e17112 (2017).
19. Z. C. Zhang, Z. You, and D. P. Chu, Light Sci. Appl. **3**, e213 (2014).
20. C. C. Zhang, Y. L. Hu, W. Q. Du, P. C. Wu, S. L. Rao, Z. Cai, Z. X. Lao, B. Xu, J. C. Ni, J. W. Li, G. Zhao, D. Wu, J. R. Chu, and K. Sugioka, Sci. Rep. **6**, 33281 (2016).
21. M. Malinauskas, A. Žukauskas, S. Hasegawa, Y. Hayasaki, V. Mizeikis, R. Buividas, and S. Juodkazis, Light Sci. Appl. **5**, e16133 (2016).
22. J. Zhang, M. Gecevičius, M. Beresna, and P. G. Kazansky, Phys. Rev. Lett. **112**, 033901 (2014).
23. M. Silvennoinen, J. Kaakkunen, K. Paivasaari, and P. Vahimaa, Phys. Procedia **41**, 693 (2013).
24. J. Bengtsson, Appl. Opt. **33**, 6879 (1994).
25. Z. Kuang, W. Perrie, J. Leach, M. Sharp, S. P. Edwardson, M. Padgett, G. Dearden, and K. G. Watkins, Appl. Surf. Sci. **255**, 2284 (2008).
26. S. Hasegawa, H. Ito, H. Toyoda, and Y. Hayasaki, Opt. Express **24**, 18513 (2016).
27. Z. Kuang, W. Perrie, D. Liu, S. Edwardson, J. Cheng, G. Dearden, and K. Watkins, Appl. Surf. Sci. **255**, 9040 (2009).
28. J. P. Vizcaíno, O. Mendoza-Yero, R. Borrego-Varillas, G. Mínguez-Vega, J. R. V. de Aldana, and J. Lancis, Opt. Lett. **38**, 1621 (2013).
29. R. Buividas, S. Rekštytė, M. Malinauskas, and S. Juodkazis, Opt. Mater. Express **3**, 1674 (2013).
30. B. Chimier, O. Utéza, N. Sanner, M. Sentis, T. Itina, P. Lassonde, F. Légaré, F. Vidal, and J. C. Kieffer, Phys. Rev. B **84**, 094104 (2011).
31. V. Koubassov, J. F. Laprise, F. Théberge, E. Förster, R. Sauerbrey, B. Müller, U. Glatzel, and S. L. Chin, Appl. Phys. A **79**, 499 (2004).
32. A. Marcinkevicius, S. Juodkazis, M. Watanabe, M. Miwa, S. Matsuo, H. Misawa, and J. Nishii, Opt. Lett. **26**, 277 (2001).
33. C. S. Lim, M. H. Hong, A. S. Kumar, M. Rahman, and X. D. Liu, Int. J. Mach. Tools Manuf. **46**, 552 (2006).